16th World Conference on Earthquake Engineering, 16WCEE 2017

Santiago Chile, January 9th to 13th 2017

Paper N° 1372 (Abstract ID)

Registration Code: S-Y1463693650

QUASI-STATIC TESTING OF A LARGE-SCALE BRIDGE WITH DISSIPATIVE CONTROLLED ROCKING CONNECTIONS IN THE SUPERSTRUCTURE

Z. Chegini[(1)], A. Palermo[(2)]

[(1)] *PhD Candidate, University of Canterbury, zeinab.chegini@pg.canterbury.ac.nz*
[(2)] *Associate Professor, University of Canterbury, alessandro.palermo@canterbury.ac.nz*

Abstract

Accelerated bridge construction techniques have gained popularity in recent years since they offer many advantages compared to traditional in-situ methods. Such advantages include rapid construction, higher quality concrete, improved work zone safety and minimal traffic disruption. Application of these methods in seismic areas is however currently limited due to a requirement for reliable connections between prefabricated elements that can provide sufficient ductility. The research presented herein aims to address this issue by introducing a hybrid rocking low-damage connection for precast bridge superstructures.

A simply supported bridge traditionally uses a combination of shear keys between the superstructure and steel linkages to provide transverse support to the superstructure and to prevent unseating of the spans during earthquake loading. The proposed connection adds longitudinal post-tensioning in combination with axial dissipaters to the superstructure to achieve a deck rocking motion with self-centering and dissipative capabilities respectively given by the un-bonded post-tensioned cables and dissipater. As a result adjacent superstructure segments aid each other in countering the transverse seismic load, rather than merely relying on the shear keys to do so. This method is an alternative solution to seismic isolation, leading to low transmission of forces to the superstructure and protection of the bridge.

This paper presents the results of quasi-static tests performed on a 1:3 scaled concrete bridge specimen with a length, width and height of 10, 3 and 4 meters respectively. Low-damage hybrid connections were the superstructure and the specimen was subjected to loading in the transverse direction. The two hollow-core decks of this short-span, two-bay bridge were connected using post-tensioning tendons, and mild steel dissipaters linked the two superstructure spans to increase energy dissipation. The testing was carried out using different values of initial post-tensioning in the tendons with and without the dissipaters and the results were compared. The specimen showed promising results in terms of self-centering and dissipation; both which can improve the performance of the bridge during seismic loading.

Keywords: low-damage; dissipative controlled rocking; prefabrication; accelerated bridge construction; ABC

1. Introduction

Prefabrication of bridge superstructures is a method commonly used to reduce construction time, offer higher construction quality and improve work-zone safety. Traditionally a concrete bridge superstructure is either designed to be monolithic with the cap beam and abutments through a moment resisting connection or is simply supported through bearings. Numerous failures of bridges using the latter type of connection have been observed under seismic loading, including unseating of the superstructure [1] and damage to the cap beam or abutment shear keys [2]. This behaviour can be controlled to some extent by increasing the seating length and connecting adjacent sections of the superstructure together using steel linkages [3].

In this paper a connection is proposed that uses unbonded longitudinal post-tensioning and mild steel dissipaters as a way of improving the behaviour of simply supported superstructures under seismic loading. The post-tensioning provides a self-centering capability and reduces the residual deformation in the connection, which in combination with the mild steel dissipaters results in a hysteretic behaviour characterized by flag-shaped loops for the connection in which it is used (Figure 1). This connection was originally developed for use in precast concrete frames [4] and later used in shear walls and bridge piers [5, 6, 7, 8]. Unlike traditional monolithic joints, which are designed to provide ductility and dissipation through plastic hinging, the hybrid connection allows for the inelastic demand to be accommodated outside the precast elements (in the mild steel or dissipation devices) while other parts of the seismic-resisting structure remain elastic and relatively intact. This improves overall performance of the bridge and prevents unseating of the superstructure.

When this connection is used between superstructure spans, it can provide a re-centering moment as well as increase dissipation during lateral transverse seismic motion (Figure 2). This results in an improvement in the overall performance of the bridge and prevents unseating of the superstructure. In this paper the results from a series of quasi-static tests on a 1:3 scaled concrete bridge specimen using described hybrid connections in the superstructure are presented.

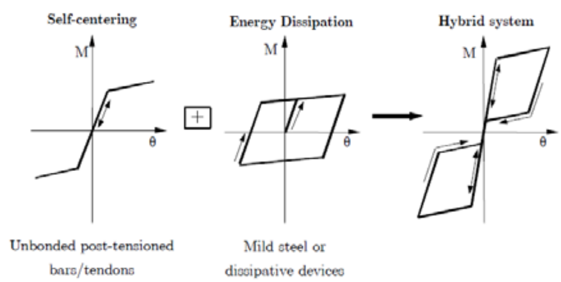

Fig. 1 – Combination of post-tensioning and dissipation yields ideal flagshape behaviour [11]

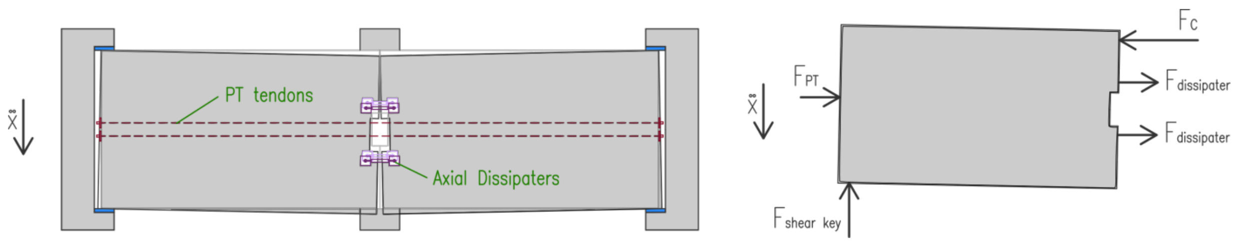

Fig. 2 – Application of dissipative controlled rocking to a bridge superstructure. F_c is the compressive force from the concrete, whereas $F_{dissipater}$ and F_{PT} are the tensile forces in the dissipaters and post-tensioning, respectively. $F_{shear\ key}$ is the reaction of the abutments to the transverse seismic force which is transferred to the superstructure through the shear keys.

3. Experimental testing

3.1 Prototype bridge

The prototype structure, which the test specimen was based on, is representative of a typical short-span concrete highway bridge in New Zealand (Figure 3). A span length of 13m and a width of 10.35m (one lane in each direction) was considered for this bridge. The superstructure was selected to represent the double hollow-core section as described in NZTA Research Report 364 [9]. This section is composed of multiple smaller precast concrete hollow-core segments which are assembled together using transverse post-tensioning. Each span of the bridge is supported by a pier cap beam connected to a circular pier with a diameter of 1.5m. The center of mass of the super structure is located 7m above the base of the pier. The footings shown are for indicative purposes only. The prototype bridge is assumed to have an importance level equal to normal, and is located in Christchurch with a zone factor of 0.3, soil type C and no near field effects. A ductility of 3 was adopted for design with a drift of %2.7.

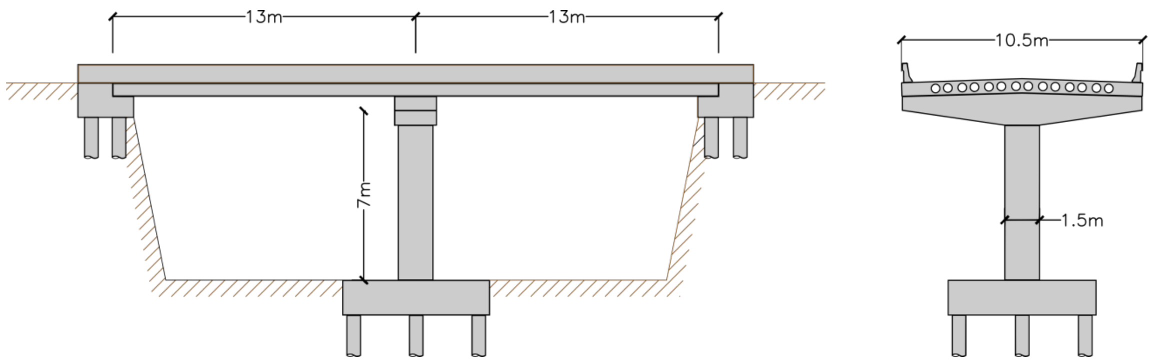

Fig. 3 – Prototype bridge which the specimen was based upon

3.2 Specimen details

The test specimen was a 1:3 scaled model of the prototype bridge. The precast concrete components of the specimen were manufactured off-site before being transported and assembled at the Structures Extension Laboratory at the University of Canterbury. These components consisted of 2 abutments, 4 rectangular columns which represented the abutment piles, a foundation for the central pier, a central circular pier, a rectangular cap beam and two hollow core superstructure spans. In order to facilitate manufacturing and assembly of the superstructure the hollow-core slabs were cast as one piece rather than in smaller segments. PVC pipes were used to provide the hollow cores in the slabs.

Assembly of the specimen started from the rectangular piles which were erected on rectangular steel foundations. The protruding longitudinal reinforcement at the bottom of each pile was welded to a base plate which was in turn bolted to steel foundations connected to the strong floor. A 32mm MacAlloy bar was used to post-tension each pile to 150kN. This was done in order to decrease the tensile stresses in the concrete and increase the bending moment capacity of the piles. The protruding longitudinal reinforcement of each pile (8×25mm Reidbars) at the top was grouted into corresponding ducts inside the abutments to create moment-resisting connections (Figure 5-c). In order to further increase the lateral stiffness of the abutment-pile combination, the piles were braced using 25mm diameter Reidbraces (Figure 4-d).

Assembly of the central part of the substructure began by attaching the precast concrete foundation to the strong floor using bolts, and erecting the circular pier on top followed by the cap beam. The foundation, pier and cap beam were then connected using a 40mm MacAlloy bar which was later post-tensioned to 700kN. Two dowel bars measuring 600mm in length connected the pier and cap beam on either side of this post-tensioning to prevent their relative rotation. At the bottom of the pier four 25mm threaded bars connecting the pier to the foundation provided a similar restraint.

The superstructure was simply supported by the abutments and cap beam. The external shear keys on the abutments provided lateral restraint for the superstructure in the transverse direction (Figure 2). Elastomeric bearings of type IRHD60 with a thickness of 25mm were placed vertically between each superstructure segment and corresponding shear key on the abutment to prevent stress concentration and damage to the abutment. Since the aim in this stage of testing was to monitor the response of the superstructure to transverse forces, no shear keys linked the superstructure and the cap beam. The superstructure was post-tensioned in the longitudinal direction using two 15.2mm post-tensioning tendons that passed through the existing ducts in the hollow-core concrete section. A 100mm gap separated the end of each deck and the adjacent abutment. This was to provide sufficient allowance for the rotation of the deck, which would otherwise press against the abutment either causing damage or forcing it to displace in the longitudinal direction of the bridge. In practice this gap can be bridged using methods similar to those used in deck joints, such as link slabs which are constructed using engineered cementitious composites [10] and will allow for considerable deformation with minimal damage.

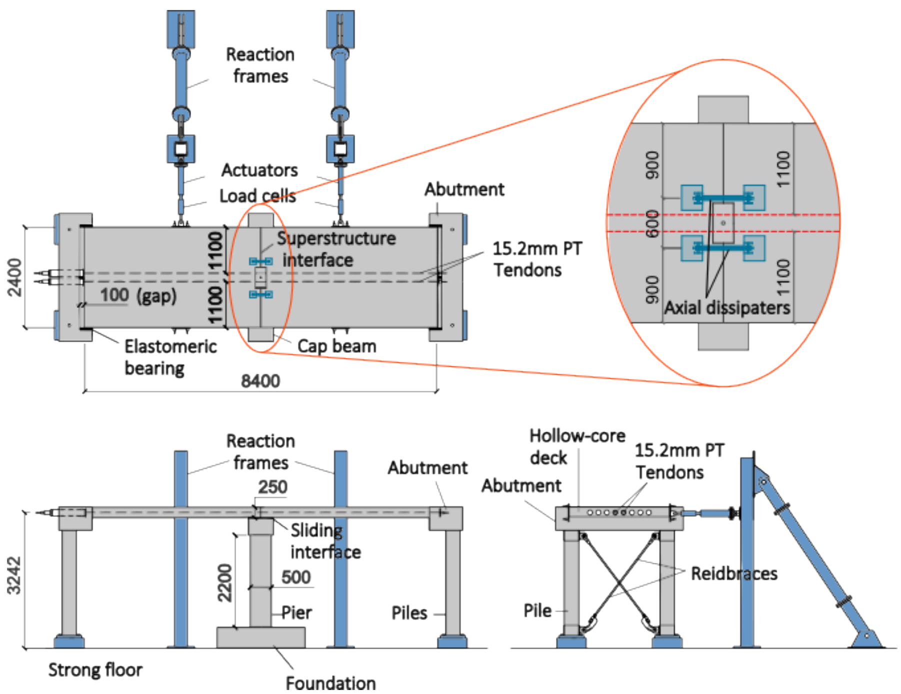

Fig. 4 – Setup and dimensions of test specimen

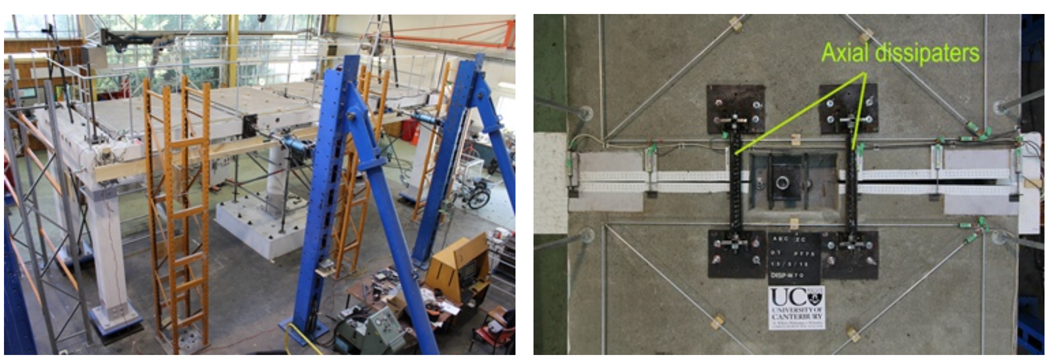

a) b)

Fig. 5 – a) View of constructed specimen, b) Axial dissipater locations

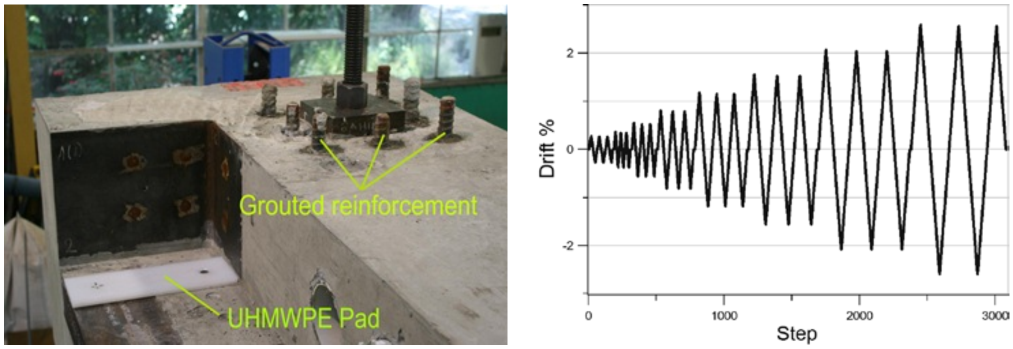

a) b)

Fig. 6 – a) UHMPWE pad on abutment, b) loading protocol used for testing

3.3 Dissipater details and material properties

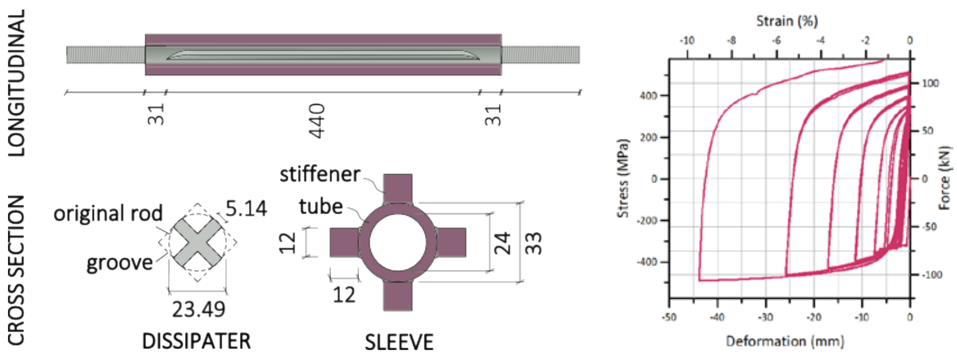

a) b)

Fig. 7 – a) Dissipater geometry, b) Force-deformation behaviour of dissipater

The dissipaters used for the testing were manufactured using Grade 300 mild steel, with a cross sectional area of 215 sqmm. The dissipaters were confined in a steel tube reinforced with stiffeners to prevent buckling, and were then connected to the bridge deck using steel brackets and bolts.

The material properties used in constructing the specimen are shown in Table 1.

Table 1– Material properties

Material	**f (MPa)**	**E (GPa)**
Concrete	f_c' = 38	27.365
Mild steel - rebars	f_y = 500 f_u = 600	210
Mild steel – dissipaters	f_y = 350 f_u = 380	210

Table 2– Properties of post-tensioning tendons

Component	Diameter (mm)	Nominal Cross-section (mm^2)	F_y (kN)	F_u (kN)	E (GPa)
VSL post-tensioning steel tendon	15.3	140	229	260	195
MacAlloy post-tensioning	32	847	670 kN	828 kN	170
MacAlloy post-tensioning	40	1320	1295 kN	1050 kN	170

3.4 Test setup and loading protocol

The test setup and loading protocol are shown in Figures 4-6. Transverse loading was applied at the deck level using two rams mounted onto reaction frames. The force was applied to the centre of each deck causing them to rotate in opposite directions. The corners of the decks were armoured using steel plates with a thickness of 6-10mm to prevent spalling in areas of stress concentration. The decks were allowed to slide on the cap beam and in order to reduce friction between the sliding surfaces UHMWPE plates were attached to the top of the cap beam and abutments in such a way that the armoured areas of the deck were supported by these raised sections (Figure 6-a).

The loading protocol was based on ACI ITG-5.1-07 [12] where the maximum force applied to the structure in the first three cycles should not exceed 60% of the design strength and the maximum displacement of the subsequent cycles should be between 1.25 and 1.5 times the maximum displacement in the previous cycles (Figure 6-b). Due to existing friction between the superstructure and bearing pads, supplementary gravity loading would affect the results of the testing and increase the amount of transverse loading for a given displacement. However this increase in force is dependent on the bearing properties and can be minimized by using bearings with a lower friction coefficient. It also does not affect the overall pattern of the force-displacement diagram and its effects can be considered by modifying the original relationship by addition of a coulomb friction force-displacement hysteretic diagram (as will be seen in section 4). Therefore no supplementary gravitational forces were used in the test setup.

Table 3– Overview of the various testing setups

Test	Post-tensioning force (total-kN)	Axial dissipaters	Friction
A	120	-	No
B	120	-	Yes
C	150	-	Yes
D	150	2	Yes

Four tests using different configurations of the specimen were selected to be presented in this paper. The configuration used for test A differed from the other configurations in that the weight of the superstructure was party supported by a crane instead of the cap beam. This was done in order to identify the effect of friction between the superstructure as it slid on the cap beam.

In configurations B and C, each of the two longitudinal tendons in the superstructure were post-tensioned to 60 and 75 kN respectively (resulting in a 120 and 150kN force in total) and no axial dissipaters were used. The setup of test D was similar to that of test C, however two axial dissipaters with a cross-section of 215 sqmm and fuse length of 440mm each attached the adjacent spans of the superstructure and were placed 900mm from the edge (Figure 5-b).

4. Results and discussion

The results of the first, second and third tests (Figures 8-10) show the multiple phases of the superstructure's response to lateral transverse loading. The first phase occurs from zero displacement until the specimen has reached a 0.7% drift ratio and represents rigid body translation or sliding of the superstructure relative to the supports. This can be seen in the force-displacement plots as segments of very low stiffness, and results from compression of the elastomeric bearings protecting the abutment shear keys. The second phase commences after the bearings reach their full compression at 0.6% drift when the superstructure segments begin to rotate and the gap between them starts to open. This is followed by the third phase, in which the gradient of the force-displacement plot is a representation of the increase in post-tensioning forces and resultant re-centering moment as the tendons are stretched further due to the gap opening.

Comparing the results of the first and second test show that the area encompassed by the moment-rotation plot is a result of friction between the cap beam and superstructure, as this area is almost equal to zero in the first test. One of the aims in using hybrid connections is minimizing residual displacements which can be achieved by choosing an appropriate ratio between post-tensioning (re-centering) and dissipative forces in the connection (Figure 1). However it can be seen from Figure 9-a that after each loading cycle the superstructure does not relocate to its neutral position of zero drift. This can be attributed to the friction mentioned above. This effect can also be seen in the results of the other tests (Figures 9, 10).

A side-by-side comparison between the results of the second and third tests shows that increasing the post-tensioning level in the superstructure's longitudinal tendons increases the lateral stiffness of the superstructure prior to gap opening but has no such effect afterwards (Figures 9, 10).

The results of the final test show a promising flag shaped hysteresis loop which confirm the self-centering and energy dissipation properties of the hybrid superstructure (Figure 11). It will be possible to achieve a higher self-centering to dissipation ration by increasing the amount of post-tensioning in the tendons and also reducing the friction between the superstructure and cap beam.

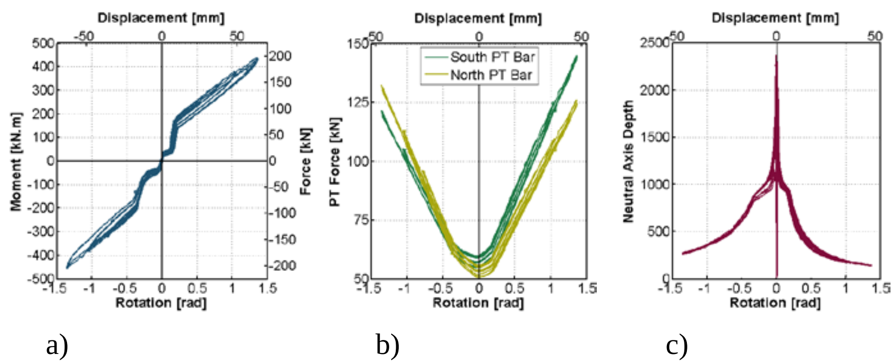

Fig. 8 – Test A, a) Moment-rotation plot of superstructure, b) Force in PT tendons c) Distance of neutral axis in superstructure from Northern edge of superstructure

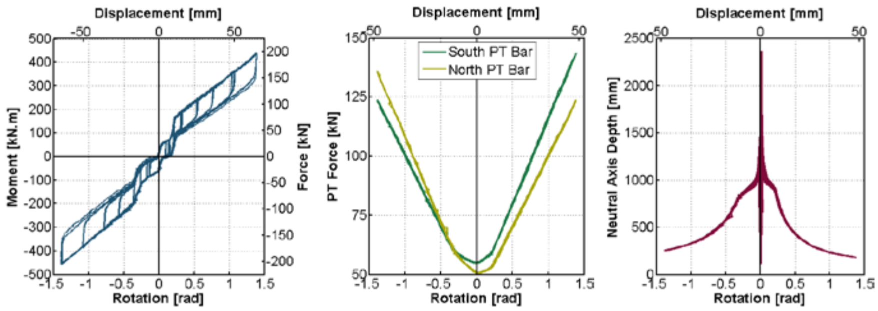

a) b) c)

Fig. 9 – Test B, a) Moment-rotation plot of superstructure, b) Force in PT tendons c) Distance of neutral axis in superstructure from Northern edge of superstructure

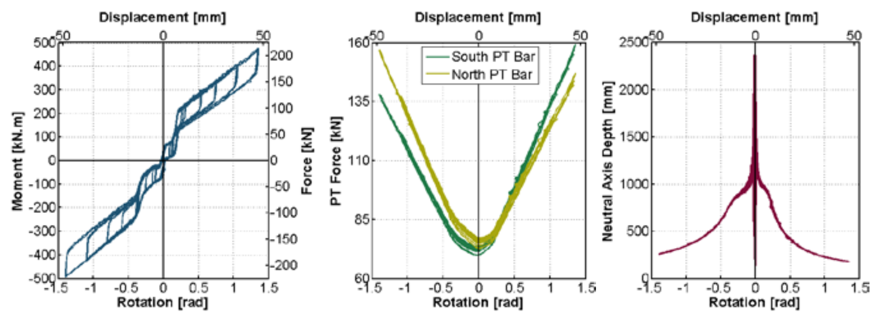

a) b) c)

Fig. 10 – Test C, a) Moment-rotation plot of superstructure, b) Force in PT tendons c) Distance of neutral axis in superstructure from Northern edge of superstructure

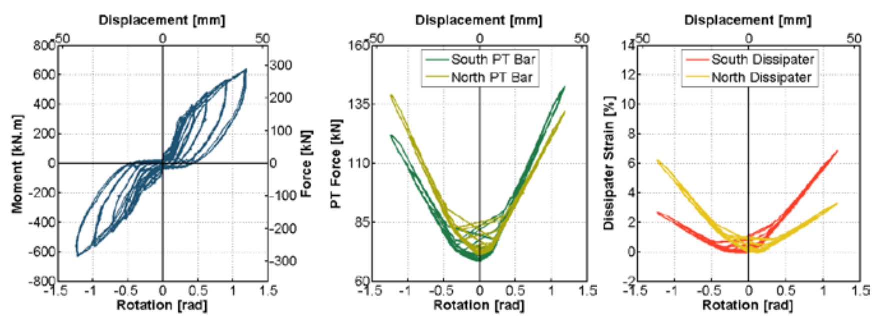

Fig. 11 – Test D, a) Moment-rotation plot of superstructure, b) Force in PT tendons c) Distance of neutral axis in superstructure from Northern edge of superstructure

5. Conclusions

Despite their many advantages the use of prefabricated bridges is still limited in seismic areas due to the need for reliable connections that offer sufficient ductility. This paper presented the findings of an experimental testing program on a 1:30 scale prefabricated concrete bridge with hybrid connections between the superstructure spans. The specimen was pre-fabricated, assembled and tested in the lateral transverse direction using a quasi-static method. The specimen showed promising results in terms of self-centering and dissipation, both which can improve the performance of the bridge during seismic loading. If used in combination with shear keys between the superstructure and cap beam, this connection can contribute to the lateral stiffness of the bridge system in addition to prevention of unseating of simply-supported superstructures and damage to shear keys in a seismic event.

4. Acknowledgements

The authors would like to express their gratitude to the Natural Hazards Research Platform (NHRP) for supporting this research as part of the project ABCD. The authors also wish to thank Bradford Building Ltd and Complete Reinforcing for their sponsorship of this project and manufacturing of the concrete specimen. The authors are thankful to technicians Gavin Keats, Russell McConchie, Peter Coursey and Alan Poynter at the Structures Extension Lab at the University of Canterbury for their contribution to the project.

5. References

[1] Buckle I, Hube M, Chen G, Yen WH, Arias J (2012): Structural performance of bridges in the offshore Maule earthquake of 27 February 2010. *Earthquake Spectra*, **28**(SUPPL.1), S533–S552.

[2] Megally SH, Silva PF, Seible F (2002): Seismic response of sacrificial shear keys in bridge abutments, *NCSD Report SSRP 2001/23*, University of California, San Diego

[3] Wood JH, Chapman HE (2013): Performance of linkage bars for restraint of bridge spans in earthquakes. *Bulletin of the New Zealand Society for Earthquake Engineering.* **46**(1), 25–39.

[4] Priestley MJN, Sritharan SS, Conley JR, Pampanin S (1999): Preliminary results and conclusions from the PRESSS five-story precast concrete test building. *PCI Journal*, **44**(6), 42–67.

[5] Palermo A, Pampanin S, Marriott D (2007): Design, modelling, and experimental response of seismic resistant bridge piers with posttensioned dissipating connections. *Journal of Structural Engineering*, **133**(11), 1648–1661.

[6] Mander JB, Cheng CT (1997): Seismic resistance of bridge piers based on damage avoidance design, *Technical Report NCEER 97-0014*. National Centre for Earthquake Engineering Research, State University of New York, Buffalo

[7] Marriott D J, Pampanin S, Palermo A (2009): Quasi-static and pseudo-dynamic testing of unbonded post-tensioned rocking bridge piers with external replaceable dissipaters. *Earthquake Engineering & Structural Dynamics*, **38**(3), 331–354. doi:10.1002/eqe.857

[8] Mashal M, White S, Palermo A (2013). Investigation of Seismic Performance of Controlled and Low Damage Rocking Systems for Accelerated Bridge Construction of Segmental Bridge Piers. *Proceedings of the Seventh National Seismic Conference on Bridges and Highways*. Oakland, California.

[9] NZ Transport Agency (2008): Standard precast concrete bridge beams.

[10] Li VC, Lepech M, Li M (2005): Field demonstration of durable link slabs for jointless bridge decks based on strain-hardening cementitious composites, Michigan Department of Transportation report no. RC-1471

[11] fib fédération internationale du béton (2003): Seismic Design of Precast Concrete Buildings, State of the Art Report. *Bulletin n. 27*

[12] ACI Innovation Task Group 5 (2008): *Acceptance criteria for special unbonded post-tensioned precast structural walls based on validation testing and commentary : an ACI standard*. Farmington Hills, Mich., American Concrete Institute.